scientific reports

OPEN

Quantum teleportation via a hybrid channel and investigation of its success probability

Seyed Mohammad Hosseiny✉, Jamileh Seyed-Yazdi✉ & Milad Norouzi

Quantum teleportation enables the transfer of quantum states across any distance and plays a prominent role in quantum communication. In this paper, we theoretically investigate the feasibility of quantum two-qubit teleportation through a hybrid channel consisting of thermal, magnetic, and local components. To study this process, we check the success probability of quantum teleportation and address the quality of the teleported quantum state using fidelity and average fidelity concepts. Furthermore, we examine a crucial quantum aspect of the system, such as the non-Markovianity of the dynamics, by utilizing success probability witness related to the teleported state. Our findings show that this hybrid channel has a good potential to be successful in quantum teleportation.

Abbreviations

Alice	Sender
Bob	Receiver
NMR	Nuclear magnetic resonance
DM	Dzyaloshinskii-Moriya interaction
KSEWA	Kaplan-Shekhtman-Entin-Wohlman-Aharony interaction
SP	Success probability
TD	Trace distance
HSS	Hilbert-Schmidt speed
CSS	Classical statistical speed
POVM	Positive operator-valued measure
QSS	Quantum statistical speed
f	Fidelity
f_{av}	Average fidelity
CT	Classical threshold

One key protocol in quantum information is quantum teleportation, which is used to transmit a quantum state[1–3]. By utilizing entanglement as a physical resource, quantum teleportation plays a crucial role in various quantum information tasks and serves as a fundamental component of quantum technologies. It plays a key role in the advancement of quantum communication[4], quantum computing[5], and quantum networks[6,7]. In principle, quantum teleportation which was first proposed by Bennett and et. al.[1], refers to a method to transfer quantum information from a sender (Alice) at one location to a receiver (Bob) some distance away sharing a classical or non-classical channel[8–12]. The quantum information that is transmitted, for instance, could be an unknown quantum state where the information is encoded in the phase of its initial state[11,12].

Today, quantum teleportation is recognized as a vital tool for various quantum protocols. So, for example, measurement-based quantum computing[13], quantum repeaters[14], and fault-tolerant quantum computation[15]. This process has been implemented in laboratories the world over employing many different substrates and technologies, including photonic qubits (e.g., light polarisation[2,3,16–20], time-bin[21–23], dual rails on a chip[24], spin-orbit qubits[25]), nuclear magnetic resonance (NMR)[26], optical modes[27–35], atomic ensembles[36–39], trapped atoms[40–44], solid-state systems[45–48], high-frequency phonons[49], and several others[8,50–54].

Quantum communication protocols' performance can be categorized into five distinct stages[11]: quantum state preparing, channel sharing, information encoding, quantum state transmitting, and received information

Physics Department, Faculty of Science, Vali-e-Asr University of Rafsanjan, Rafsanjan, Iran. ✉email: hosseinysmohammad@gmail.com; j.seyedyazdi@gmail.com

decoding. To be communicated, quantum states need to interact with an external environment[50,55,56]. The impact of different environmental noises on quantum teleportation[57–61] has been reported.

The interaction between a system and its surrounding environment is an inevitable phenomenon. These systems are not isolated and are referred to as open quantum systems in quantum information theory[62–67]. The dynamics of open quantum systems are categorized into Markovian and non-Markovian scenarios based on the system's interaction with its environment. In Markovian dynamics, information consistently flows from the system to the environment. Conversely, in non-Markovian dynamics, information periodically returns to the system from the environment due to quantum memory effects[68–70]. In open quantum systems, quantum teleportation is affected by the kind of system evolution.

The model examined in this study for quantum teleportation is a hybrid channel[71] consisting of thermal, magnetic, and local components. Also, we consider the effect of the classical static noise on the time-evolved state of the spin system. In more detail, the hybrid channel includes a two-qubit spin state affected by a thermal and magnetic field[72]. The spin system is considered to be characterized by the Dzyaloshinskii-Moriya interaction (DM), Kaplan-Shekhtman-Entin-Wohlman-Aharony interaction (KSEWA), and the anisotropic interaction[73,74]. The above-mentioned items indicate that the two-spin system is simultaneously affected by a thermal, magnetic, and classical channel.

In Ref.[71], the quantum correlations and dynamics of coherence of a simple two-qubit Heisenberg spin state were investigated to study the symmetry of this hybrid channel. In this context, the thermal interaction picture of channels has been examined using the concept of Gibb's density matrix operations[75]. Additionally, magnetic fields have been utilized to explicitly illustrate the dynamics of quantum correlations[76]. Local channels have demonstrated their effectiveness for information transmission over the years[77]. On the other hand, non-local channels have been explored, and significant efforts have been made recently to enhance their practical applications[78]. Classical channels, in contrast to non-local channels, offer the advantage of easy implementation without requiring intricate designs. However, pure classical channels are susceptible to various flaws and disturbances, such as the influence of surface charge carriers[79], and electronic currents[80], among others.

In this paper, we address the two-qubit quantum teleportation via a hybrid channel consisting of a two-qubit spin state influenced by a thermal and magnetic field under DM interaction, KSEWA interaction, and the anisotropic interaction by considering the classical static noise. To investigate the feasibility of quantum two-qubit teleportation through a hybrid channel, we examine the success probability (SP)[69] of the process and evaluate the quality of the teleported quantum state by fidelity (f) and average fidelity (f_{av}) criteria. Moreover, we analyze the non-Markovianity of the system dynamics, using several important well-known witnesses associated with the teleported state like the trace distance (TD)[68,69,81], success probability, and fidelity[82]. The applications of the results of this work can be mentioned in the practical implementation of improved quantum teleportation. The key element in quantum teleportation is the quantum channel. Consequently, numerous approaches have been explored to implement and evaluate efficient channels for this purpose. In this work, we assess a hybrid channel for quantum teleportation that has not yet been addressed in the quantum communication literature. Additionally, we propose a novel method to easily detect non-Markovian effects and the influence of quantum memory by analyzing the success probability of quantum teleportation. This concept could pave the way for new research into the dynamics of open quantum systems.

The paper's structure consists of four parts: Following the introduction, the preliminaries of quantum teleportation are outlined in Sec. 2. In Sec. 3, the theoretical model is presented as a resource for quantum teleportation. Lastly, Sec. 4 concludes by summarizing and discussing the key findings.

## Preliminaries
Quantum teleportation

To better comprehend the process of quantum teleportation, we initially offer a concise explanation. Consider the quantum teleportation protocol between Alice and Bob, who are spatially separated and simultaneously share two qubits (A and B) prepared in a pure entangled state (as shown in Fig. 1)[1,8,83]. In the ideal protocol, this is considered maximally entangled, for example, $|\Phi\rangle = \frac{1}{\sqrt{2}}\left(|00\rangle + |11\rangle\right)$ which is known as a Bell pair.

At the input, Alice is given an additional qubit (a) with an unknown state ρ_{in}. Then, Alice applies a joint quantum measurement (well-known Bell detection), which projects her qubits a and A into one of the four Bell states $(\mathcal{P}_k \otimes I)|\Phi\rangle$ with $k = 0, ..., 3$ where $\mathcal{P}_k$ and I represent a qubit Pauli operator and identity matrix, respectively. Hence, the state of Alice's input qubit has been changed due to measurement while Bob's qubit (B) is simultaneously projected onto $\mathcal{P}_k^\dagger \rho_{in} \mathcal{P}_k$. Note that, this process preserves the no-cloning theorem of quantum mechanics[84]. In the next stage, Alice transfers the classical outcome k of her measurement to Bob. In the final step of the process, Bob performs $\mathcal{P}_k$ (conditional unitary) to recover the original input state ρ_{in}.

Some components, such as the Bell measurement and unitary transformation, are essential for quantum teleportation. However, the approach to achieving teleportation may vary when different setups are implemented.

In the standard protocol[85], the remote transmission is achieved using a two-qubit mixed state ρ_{ch}, acting as a channel or resource, and is prepared by a generalized depolarized quantum channel $\Lambda(\rho_{ch})$, according to a two-qubit input state ρ_{in}. Alice intends to transmit the encoded two-qubit state to Bob using this method. One can assume the unknown input (initial) state of teleportation for an arbitrary pure two-qubit state as:

$$|\psi_{in}\rangle = \cos\left(\frac{\theta}{2}\right)|10\rangle + e^{i\phi}\sin\left(\frac{\theta}{2}\right)|01\rangle, \tag{1}$$
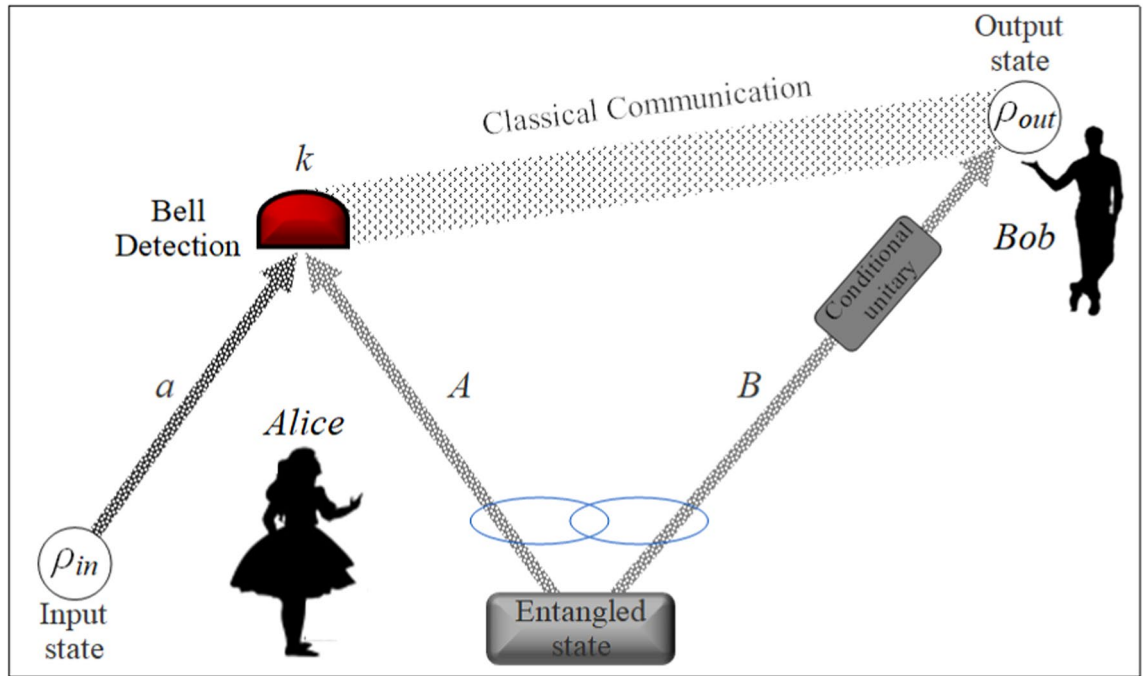
Figure 1. The schematic of the quantum teleportation protocol.

in which θ and ϕ are the amplitude and phase of the initial state of teleportation, respectively. In the transfer of an arbitrary two-qubit state (input state $\rho_{in} = |\psi_{in}\rangle\langle\psi_{in}|$)), one can define the output state of the teleportation as[57,86]:

$$\rho_{out} = \sum_{i,j=0}^{3} p_{ij}\left(\sigma_i \otimes \sigma_j\right)\rho_{in}\left(\sigma_i \otimes \sigma_j\right). \tag{2}$$

where $\sum p_{ij} = 1$ and $p_{ij} = Tr[\mathcal{B}_i\rho_{ch}]Tr[\mathcal{B}_j\rho_{ch}]$. that $\Lambda(\rho_{ch})$ represents a generalized depolarized channel and $\mathcal{B}_i$ denotes the Bell state corresponding to the Pauli matrix σ_i and is given by:

$$\mathcal{B}_i = \left(\sigma_0 \otimes \sigma_i\right)\mathcal{B}_0\left(\sigma_0 \otimes \sigma_i\right), \quad i = 1, 2, 3, \tag{3}$$

in which $\sigma_0 = \mathbb{I}, \sigma_1 = \sigma_x, \sigma_2 = \sigma_y, \sigma_3 = \sigma_z$ and $\mathbb{I}$ represents the identity matrix. Moreover, for any two arbitrary qubits, each given in base $\{|0\rangle, |1\rangle\}$, we have $\mathcal{B}_0 = \frac{1}{2}\left(|00\rangle + |11\rangle\right)\left(\langle00| + \langle11|\right)$.

The similarity between the input state and the teleported state can be assessed using the fidelity criterion. Therefore, the quality of the teleported state is determined by the fidelity $f\left(\rho_{in}(t), \rho_{out}(t)\right)$, which is given by[84,87]:

$$f\left(\rho_{in}(t), \rho_{out}(t)\right) = \left(Tr\left(\sqrt{\sqrt{\rho_{in}(t)}\rho_{out}(t)\sqrt{\rho_{in}(t)}}\right)\right)^2, \tag{4}$$

where the limit for fidelity is $0 \leq f\left(\rho_{in}(t), \rho_{out}(t)\right) \leq 1$. For $f = 1$, the optimum fidelity that leads to optimum teleportation can be obtained. Furthermore, one can define the average fidelity of teleportation f_{av} as:

$$f_{av} := \frac{1}{4\pi}\int_0^{2\pi} d\phi \int_0^{\pi} f\left(\rho_{in}(t), \rho_{out}(t)\right)sin(\theta)d\theta. \tag{5}$$

Attention must be paid to the fact that the threshold of the maximum classical average fidelity is at $f_{av} = 2/3$. If $f_{av} = 1$, then, the optimum quantum teleportation can be achieved and depicts that less information is leaked.

Trace distance (TD) and success probability (SP)

The distinguishability of two evolving states of the quantum system ρ_{in} and ρ_{out}, which is one of the most well-known approaches to identifying the non-Markovianity of the system dynamics which was suggested by Breuer et al.[68,88], is trace distance (TD)[68,69,81]:

$$D\left(\rho_{in}, \rho_{out}\right) = \frac{1}{2}\mathrm{Tr}|\rho_{in} - \rho_{out}|. \tag{6}$$

where the modulus of the operator is defined by $|A| = \sqrt{A^\dagger A}$. The bounds of TD are $0 \leqslant D\left(\rho_{in}, \rho_{out}\right) \leqslant 1$, where $D\left(\rho_{in}, \rho_{out}\right) = 0$ if and only if $\rho_{in} = \rho_{out}$, and $D\left(\rho_{in}, \rho_{out}\right) = 1$ if and only if ρ_{in} and ρ_{out} are orthogonal. It can be proved that the maximum success probability (SP) Bob can achieve through an optimal strategy that is directly linked to the TD and is given by[69]:

$$\mathrm{SP}_{\max} = \frac{1}{2}\left[1 + D\left(\rho_{in}, \rho_{out}\right)\right]. \tag{7}$$

If we assume the states prepared by Alice are orthogonal such that $D\left(\rho_{in}, \rho_{out}\right) = 1$ then we have $\mathrm{SP}_{\max} = 1$ so that orthogonal states can be distinguished with certainty by a single measurement. It should be noted that we can calculate the success probability of quantum two-qubit teleportation by using Eq. 7 with the input (Eq. 1) and output (Eq. 2) states of the channel.

Hilbert-Schmidt speed (HSS) as phase estimator

Hilbert-Schmidt speed (HSS) is recognized as a potent tool for estimating the quantum parameters in quantum information theory. Assuming the quantum state $\rho(\vartheta)$, the HSS can be determined as[89–91]:

$$HSS(\vartheta) = \max_{\{\Pi_x\}} s[p(\vartheta)] = \sqrt{\frac{1}{2}\mathrm{Tr}\left[\frac{d\rho(\vartheta)}{d\vartheta}\right]^2}. \tag{8}$$

which does not require diagonalizing $d\rho(\vartheta)/d\vartheta$.

Non-Markovianity measure with respect to the information backflow based on success probability

It is well known that non-Markovian effects can lead to quicker quantum evolution from an initial state to a subsequent state[92–97]. The success probability can effectively determine memory effects in system dynamics. Here, we emphasize exploiting the success probability as a valuable witness of the non-Markovian aspect of quantum evolutions, leading to practical benefits in analysis.

Following what was reported for the trace distance in Ref.[68] and according to the formulation of the success probability (Eq. 7), another non-Markovian witness can be introduced based on the success probability SP. Regarding the idea that a nonmonotonic speed (positive acceleration) of quantum dynamics indicates memory effects in the system dynamics, a non-Markovianity witness based on SP can be introduced as

$$\mathcal{I}(t) := \frac{dSP(t)}{dt} > 0, \tag{9}$$

If the system interacts with its surrounding environment, i.e. there is a system-environment information exchange, the SP decreases monotonically, then dynamics is known as Markovian. So, we have for some time intervals $\mathcal{I}(t) < 0$. In contrast, every positive value of $\mathcal{I}(t) > 0$ denotes a witness of non-Markovianity.

According to this witness, similar to what has been done for other measures[68,82,88,91,98], a determiner of the degree of non-Markovianity can be defined as

$$\mathcal{N} := \max \int_{\mathcal{I}(t)>0} \mathcal{I}(t)dt, \tag{10}$$

where the maximization is carried out over all possible parameterizations of the initial state. It is essential to note this point that in this article we evaluate the quantity presented in Eq. 10 according to the quantities of success probability, and fidelity, which expresses the degree of non-Markovian system dynamics.

Theoretical model

Consider a paradigmatic open quantum system including two-spin-1/2 of XXZ Heisenberg chain that is influenced by an external homogeneous magnetic field characterized by the Dzyaloshinskii-Moriya (DM) and Kaplan-Shekhtman-Entin-Wohlman-Aharony (KSEWA) coupling interactions along the z-direction[71,99] (as illustrated in Fig. 2). The Hamiltonian of this model in the standard basis $\{|00\rangle, |01\rangle, |10\rangle, |11\rangle\}$ can be expressed as:
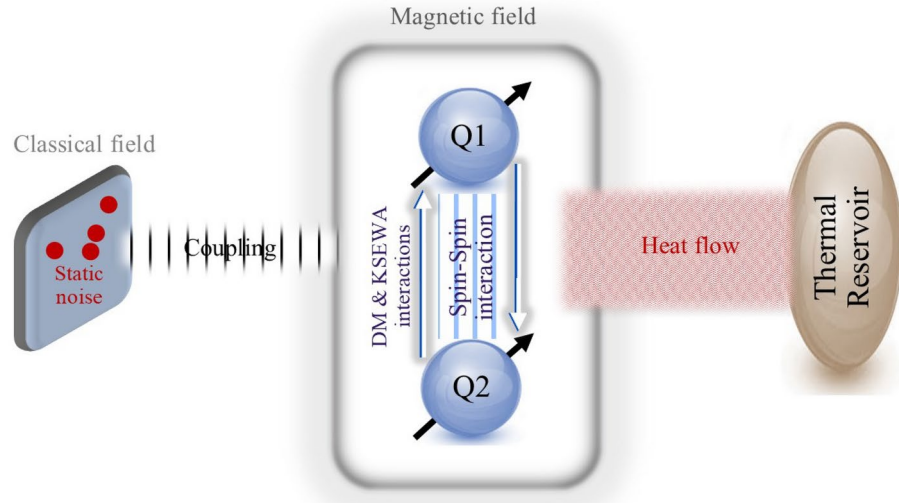
Figure 2. The physical model of the hybrid channel with thermal, magnetic, and classical dephasing parts including the two-qubit Heisenberg spin state characterized by spin-spin, DM, and KSEWA interactions under classical static noise.

$$H = \begin{pmatrix} 2B + \Delta_z & 0 & 0 & -2iK_z \\ 0 & -\Delta_z & 2iD_z + 2J & 0 \\ 0 & -2iD_z + 2J & -\Delta_z & 0 \\ 2iK_z & 0 & 0 & -2B + \Delta_z \end{pmatrix}. \tag{11}$$

in which Δ_z is the real anisotropy coupling constant depicting the symmetric exchange spin-spin interaction in the z-direction, D_z the strength of the DM interaction that regulates the spin-orbit antisymmetric coupling, and J expresses the Heisenberg exchange interaction between the spins. Furthermore, K_z denotes the KSEWA interaction strength along the z-direction corresponding to symmetric spin-orbit coupling, while B represents the homogeneous component of the assumed magnetic field.

Given Gibbs's density operator $\rho(0,T) = \frac{1}{Z}\left(\exp(-\beta H)\right) = \frac{1}{Z}\sum_n \exp(-\beta\epsilon_n)|\psi_n\rangle\langle\psi_n|$ in which $Z = \text{Tr}[\exp(-\beta H]$ represents the partition function, and $\beta = 1/(k_B T)$ (where the k_B is the Boltzmann constant with setting $k_B = 1$ and T is temperature) and considering the Hamiltonian in Eq. 11 at thermal equilibrium with a thermal reservoir at temperature T, one can determine the thermal state density matrix in terms of eigenvalues ϵ_n and eigenvectors $|\psi_n\rangle$ in the standard basis $\{|00\rangle, |01\rangle, |10\rangle, |11\rangle\}$ as follows:

$$\rho(0,T) = \begin{pmatrix} \rho_{11} & 0 & 0 & \rho_{14} \\ 0 & \rho_{22} & \rho_{23} & 0 \\ 0 & \rho_{23}^* & \rho_{33} & 0 \\ \rho_{41}^* & 0 & 0 & \rho_{44} \end{pmatrix}. \tag{12}$$

where corresponding elements of this matrix are obtained as

$$\rho_{11} = \frac{1}{Z}e^{-\frac{\Delta_z}{T}}\left(\cosh(\varphi) - \frac{B\sinh(\varphi)}{\sqrt{B^2 + K_z^2}}\right),$$

$$\rho_{14} = \rho_{41}^* = \frac{1}{Z\sqrt{B^2 + K_z^2}}iK_z e^{-\frac{\Delta_z}{T}}\sinh(\varphi),$$

$$\rho_{22} = \rho_{33} = \frac{1}{Z}e^{\frac{\Delta_z}{T}}\cosh(\omega), \tag{13}$$

$$\rho_{23} = \rho_{32}^* = \frac{1}{Z\sqrt{D_z^2 + J^2}}\left(-J - iD_z\right)e^{\frac{\Delta_z}{T}}\sinh(\omega),$$

$$\rho_{44} = \frac{1}{Z}e^{-\frac{\Delta_z}{T}}\left(\frac{B\sinh(\varphi)}{\sqrt{B^2 + K_z^2}} + \cosh(\varphi)\right),$$

in which $\varphi = \frac{1}{T}\left(2\sqrt{B^2 + K_z^2}\right), \omega = \frac{1}{T}\left(2\sqrt{D_z^2 + J^2}\right)$ and | partition function is $Z = 2e^{-\frac{\Delta_z}{T}}\left(e^{\frac{2\Delta_z}{T}}\cosh(\omega) + \cosh(\varphi)\right)$.

We apply a common classical environment characterized by static noise to the two-qubit spin state. In the current scenario, the Hamiltonian that dictates the present physical model is expressed as[71,100]:

$$H_{XY} = H_X \otimes I_Y + I_X \otimes H_Y, \quad \text{with} \quad H_k = \begin{pmatrix} \Delta_k \lambda + \epsilon & 0 \\ 0 & \epsilon - \Delta_k \lambda \end{pmatrix}, \tag{14}$$

in which $H_k(k = X, Y)$ represents the Hamiltonian state of the sub-system k, ϵ denotes the equal energy splitting between the sub-systems, I signifies the 2×2 identity matrix, λ refers the coupling constant, Δ_k detunes the stochastic behavior of the classical field and its value is flipping between ± 1. The Hamiltonian in relation (14) commutes at different times, eliminating the need for the Dyson series[101].

To evolve the two-qubit state in the classical field, we employ the time unitary operation $U_{XY}(t) = \exp\left[-i\int_{t_0}^{t} H(z)dz\right]$

[102] with setting $\hbar = 1$. Then, the time-evolved state of the two qubits initially prepared in thermal state $\rho(0, T)$, when exposed to an identical channel, i.e., $\Delta_X = \Delta_Y$, can be calculated as:

$$\rho(t, T) = U_{XX}(t)\rho(0, T)U_{XX}^{\dagger}(t) = \begin{pmatrix} \rho_{11} & 0 & 0 & e^{-4i\Delta_X \lambda t}\rho_{14} \\ 0 & \rho_{22} & \rho_{23} & 0 \\ 0 & \rho_{32}^* & \rho_{33} & 0 \\ \rho_{41}^* e^{4i\Delta_X \lambda t} & 0 & 0 & \rho_{44} \end{pmatrix}. \tag{15}$$

Here, the impact of static noise on the time-evolved state of the spin system is discussed. Accordingly, static noise is commonly determined by Δ_Q which is the disorder parameter that has the probability distribution function $O(\delta) = 1/\Delta_Q$ and depicts the range $|\delta - \delta_0| \leq \Delta_Q^2/2$, where δ_0 represents the mean value of the probability distribution function[71,102]. In order to determine the influence of the static noise on the dynamics of the spin state, the time-evolved state density matrix was averaged over all possible noise states. Finally, one can integrate the matrix in Eq. 15 on $r^+ = \delta_0 - \Delta_Q/2$ and $r^- = \delta_o + \Delta_Q/2$ as follows[71,103]:

$$\rho_{st}(t, T) = \int_{r^-}^{r^+} \frac{1}{\Delta_Q}\rho(t, T)d\Delta_X = \begin{pmatrix} \rho_{11} & 0 & 0 & \rho_{14}\frac{e^{-4i\delta_0\lambda t}\sin(2\Delta_Q\lambda t)}{2\Delta_Q\lambda t} \\ 0 & \rho_{22} & \rho_{23} & 0 \\ 0 & \rho_{23}^* & \rho_{33} & 0 \\ \rho_{14}\frac{e^{-4i\delta_0\lambda t}\sin(2\Delta_Q\lambda t)}{2\Delta_Q\lambda t} & 0 & 0 & \rho_{44} \end{pmatrix}. \tag{16}$$

that the non-vanishing elements of this matrix also follow the same elements of relation 13. It is noteworthy that the aforementioned final density matrix shows the two-spin system simultaneously affected by a thermal, magnetic, and classical channel. In this paper, we use the final density matrix in Eq. 16 which is called a hybrid channel, as a resource or channel for quantum two-qubit teleportation.

The important point in plotting the figures is that we use the nondimensionalized parameter method throughout the work as described in[12,104]. Hence, all parameters are considered nondimensionalized.

Discussion and results

The output state of quantum two-qubit teleportation for Eq. 16 as a resource or channel of quantum teleportation, substituting Eqs. 3, 1, and 16 in 2, can be calculated as:

$$\rho_{out}(t, T) = \begin{pmatrix} \rho_{out,11} & 0 & 0 & \rho_{out,14} \\ 0 & \rho_{out,22} & \rho_{out,23} & 0 \\ 0 & \rho_{out,32} & \rho_{out,33} & 0 \\ \rho_{out,41} & 0 & 0 & \rho_{out,44} \end{pmatrix} \tag{17}$$

where non-vanishing elements of the output matrix can be given by

$$\rho_{out,11} = \rho_{out,44} = \frac{e^{\frac{2\Delta_z}{T}}\cosh(\varphi)\cosh(\omega)}{\left(e^{\frac{2\Delta_z}{T}}\cosh(\omega)+\cosh(\varphi)\right)^2},$$

$$\rho_{out,14} = -\frac{iJK_z\left(1+e^{2i\phi}\right)\sin(\theta)\sinh(\varphi)\sinh(\omega)\sin(2\Delta_Q\lambda t)e^{\frac{2\Delta_z}{T}-i(4\delta_0\lambda t+\phi)}}{\Delta_Q\lambda t T^2\varphi\omega\left(e^{\frac{2\Delta_z}{T}}\cosh(\omega)+\cosh(\varphi)\right)^2},$$

$$\rho_{out,22} = \frac{\frac{1}{2}\sin^2(\theta)\cosh^2(\varphi)+\frac{1}{2}\cos^2(\theta)e^{\frac{4\Delta_z}{T}}\cosh^2(\omega)}{\left(e^{\frac{2\Delta_z}{T}}\cosh(\omega)+\cosh(\varphi)\right)^2},$$

$$\rho_{out,33} = \frac{\frac{1}{2}\cos^2(\theta)\cosh^2(\varphi)+\frac{1}{2}\sin^2(\theta)e^{\frac{4\Delta_z}{T}}\cosh^2(\omega)}{\left(e^{\frac{2\Delta_z}{T}}\cosh(\omega)+\cosh(\varphi)\right)^2}, \quad (18)$$

$$\rho_{out,23} = -\frac{\sin(\theta)e^{-i(8\delta_0\lambda t+\phi)}\left(K_z^2\omega^2 e^{2i\phi}\sinh^2(\varphi)\sin^2(2\Delta_Q\lambda t)-4\Delta_Q^2 J^2\lambda^2 t^2\varphi^2\sinh^2(\omega)e^{\frac{4\Delta_z}{T}+8i\delta_0\lambda t}\right)}{2\Delta_Q^2\lambda^2 t^2 T^2\varphi^2\omega^2\left(e^{\frac{2\Delta_z}{T}}\cosh(\omega)+\cosh(\varphi)\right)^2},$$

$$\rho_{out,32} = \frac{\sin(\theta)e^{-i(8\delta_0\lambda t+\phi)}\left(-\frac{1}{4}K_z^2\left(T^2\omega^2\right)\sinh^2(\varphi)\sin^2(2\Delta_Q\lambda t)+\Delta_Q^2 J^2\lambda^2 t^2\left(T^2\varphi^2\right)\sinh^2(\omega)e^{\frac{4\Delta_z}{T}+2i(4\delta_0\lambda t+\phi)}\right)}{2\Delta_Q^2\lambda^2 t^2 T^2\varphi^2\omega^2\left(e^{\frac{2\Delta_z}{T}}\cosh(\omega)+\cosh(\varphi)\right)^2}.$$

Now using the output state of Eq. 17 and Eqs. 4, 5, 1, 7, and 8 we can investigate the qualitative behaviors of fidelity f, average fidelity f_{av}, success probability SP, and Hilbert-Schmidt speed with respect to initial phase HSS_ϕ for quantum two-qubit teleportation based on hybrid channel (Eq. 16).

In Fig. 3a–d, the qualitative behaviors of success probability SP, fidelity f, average fidelity f_{av}, and Hilbert-Schmidt speed with respect to the initial phase of the input state of the teleportation HSS_ϕ are shown. The significant outcomes of successful quantum teleportation via the current hybrid channel are clearly depicted in this figure. One of these outcomes is that the success probability SP of quantum teleportation in some intervals is equal to unity or close to unity. It means that the initial state has been successfully transferred from Alice to Bob. Since the TD plays a crucial role in the SP formula and well-known witness to probing the non-Markovianity
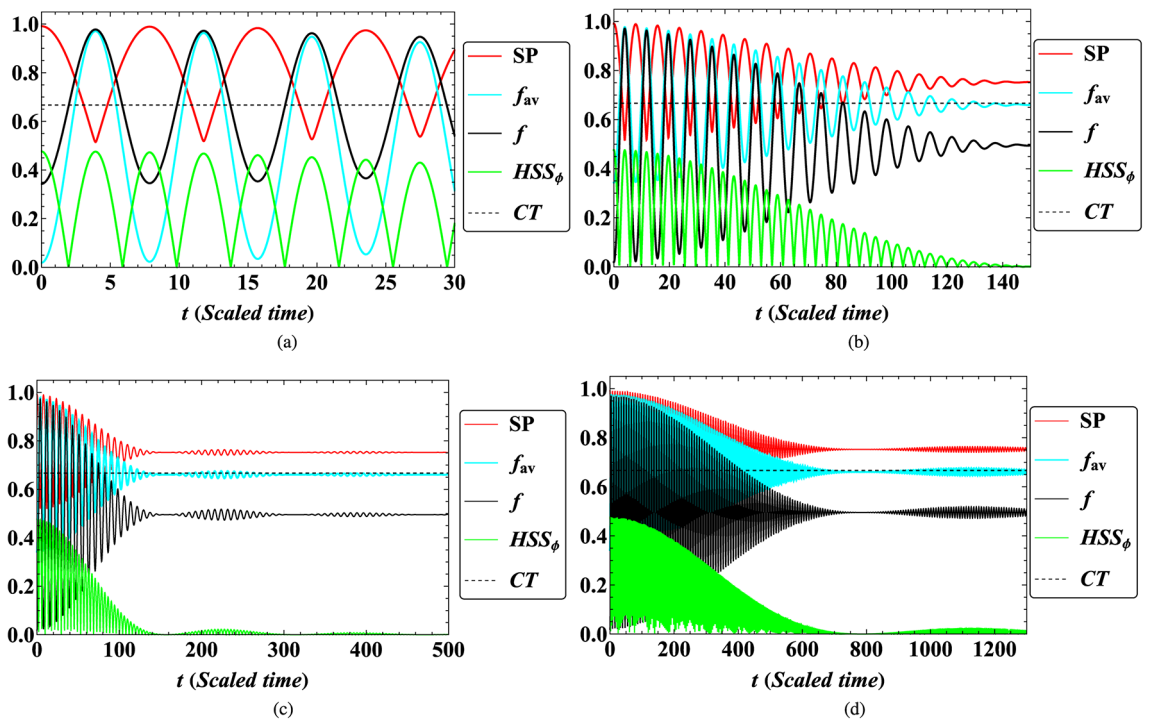

Figure 3. The comparison between the dynamics of success probability SP, fidelity f, average fidelity f_{av} and Hilbert-Schmidt speed with respect to phase HSS_ϕ in quantum two-qubit teleportation when (**a**) $B = 1, J = 1, K_z = 5, D_z = 1, \Delta_z = 1, \Delta_Q = 0.1, \lambda = 0.1\ \delta_0 = 1, \theta = \pi/2, \phi = \pi, T = 1$, (**b**) the same values of parameters in the previous term for more time, (**c**) the same values of parameters in the previous term for more time, and (**d**) $B = 1, J = 1, K_z = 5, D_z = 1, \Delta_z = 1, \Delta_Q = 0.02, \lambda = 0.1, \delta_0 = 1, \theta = \pi/2, \phi = \pi, T = 1$. Here, $CT = 2/3 \approx 0.67$ represents the classical threshold of teleportation. Note that, all parameters are nondimensionalized in plotting all figures throughout this article.

of dynamics, hence the non-Markovianity of system dynamics also can be seen in this figure. Given Eqs. (9 and 10), the non-Markovianity witness is based on the *SP* introduced. Therefore, in this figure, we can detect the non-Markovian effects for $\mathcal{I}(t) > 0$ due to quantum memory effects. Additionally, as suggested in Ref.[82], another non-Markovian witness can be introduced based on fidelity. Here we can see that fidelity and success probability behaviors are the opposite of each other. Hence, their information flows run in contrary directions. Moreover, we see that the values of the fidelity f and average fidelity f_{av} are more over than the classical threshold CT in some intervals which indicates the good quality of quantum teleportation. Furthermore, we consider that the important information has been encoded in the phase of the initial qubit state and Alice transfer the quantum state to Bob. The quantum phase estimation via HSS in quantum teleportation based on the presented model is implemented. The significant point that can be stated here is that the information at the destination of the teleportation is suppressed over time. Of course, in some intervals of time, we can see that the HSS curve recovers after the suppression of oscillations due to dephasing effects, but many times, the amount of received information is low, which indicates that in very long times (more than 450 in Fig. 3c) Bob may have problems in receiving encoded information in the initial state phase. The interesting thing is that in Fig. 3d we can see that by reducing the disorder parameter Δ_Q or static noise control parameter, Bob can still receive information for much longer times and have better quantum teleportation. This means that less noise in the classical field can bring better teleportation quality, which is in agreement with the practical view of teleportation.

Given the crucial role of the SP in quantum teleportation, our attention is directed towards the qualitative behavior of the SP. The temporal variations of the SP with increasing disorder parameter Δ_Q or static noise control parameter are illustrated in Fig. 4a–c. This figure states that by decreasing the Δ_Q, the better quality of quantum two-qubit teleportation can be achieved because of decreasing static noise of the classical field. Hence, to improve quantum teleportation we must prevent additional noise from entering the system in the current model. All Fig. 4a–c are plotted with the same parameter values. Fig. 4a,b are plotted for a better understanding of the system's behavior in different time intervals, and Fig. 4c is its contour plot. Fig. 4b shows that the SP can be obtained in more time with the setting of Δ_Q. Fig. 4c also displays the necessity of decreasing the Δ_Q to better transfer of quantum state.
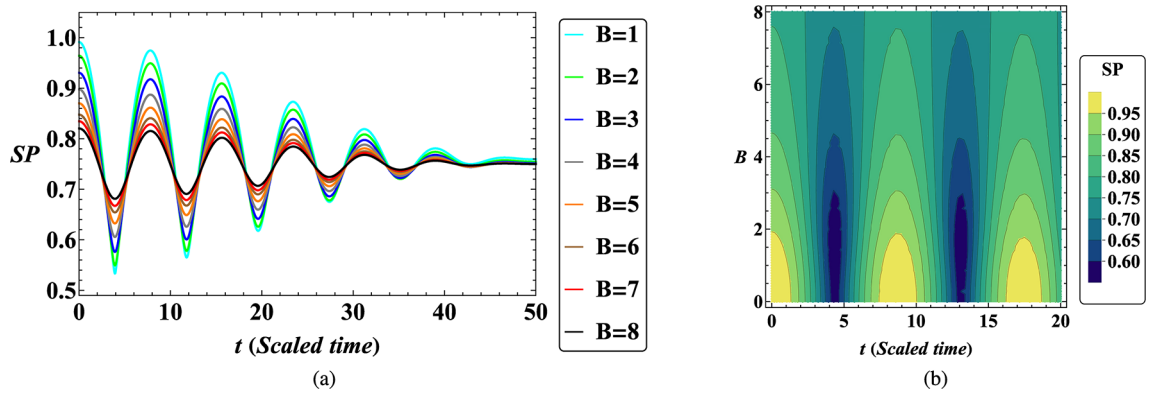
In Fig. 5, the time evolution of the SP with increasing the homogeneous component of the magnetic field B is plotted. It is clear that the qualitative behavior of the SP for quantum two-qubit teleportation based on the present channel is disturbed under increasing the homogeneous component of the magnetic field B. Hence to enhance the quality of quantum teleportation based on the hybrid channel, the external homogeneous magnetic field must be lower than order 1.

Next, in Fig. 6a, b, the qualitative behaviors of the SP with increasing the KSEWA interaction strength K_z and with increasing the anisotropy coupling constant Δ_z are presented, respectively. In Fig. 6a, as K_z increases, the qualitative behavior of the SP becomes more oscillatory, and the value of the SP approaches unity. Consequently, the quantum teleportation based on a hybrid channel is enhanced under the influence of the KSEWA interaction. Conversely, in Fig. 6b, as Δ_z rises, we observe that the qualitative behavior of the SP becomes less oscillatory, and
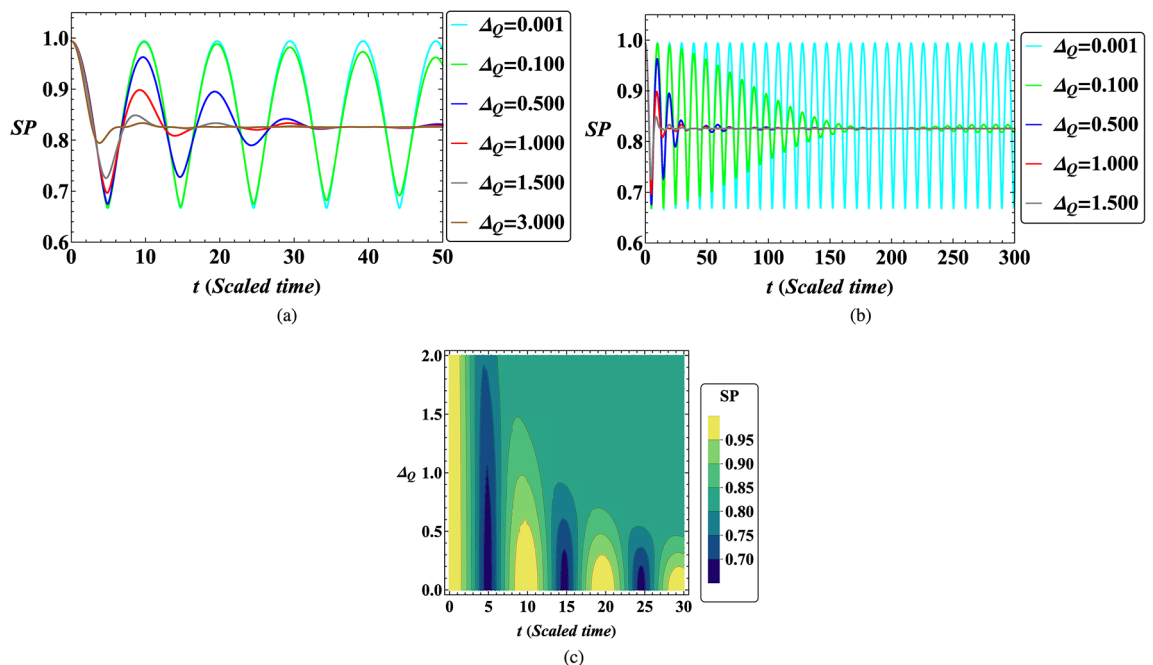

Figure 4. The temporal variations of success probability SP of quantum two-qubit teleportation with increasing disorder parameter Δ_Q (increasing static noise) when (**a**) $B = 0.6$, $J = 1.2$, $K_z = 4$, $D_z = 2$, $\Delta_z = 1$, $\lambda = 0.08$, $\delta_0 = 1$, $\theta = \pi/2$, $\phi = \pi$, $T = 1$, (**b**) the same values of parameters in the previous term for more time, and (**c**) the contour plot Δ_Q vs t with the same values of parameters in previous term.
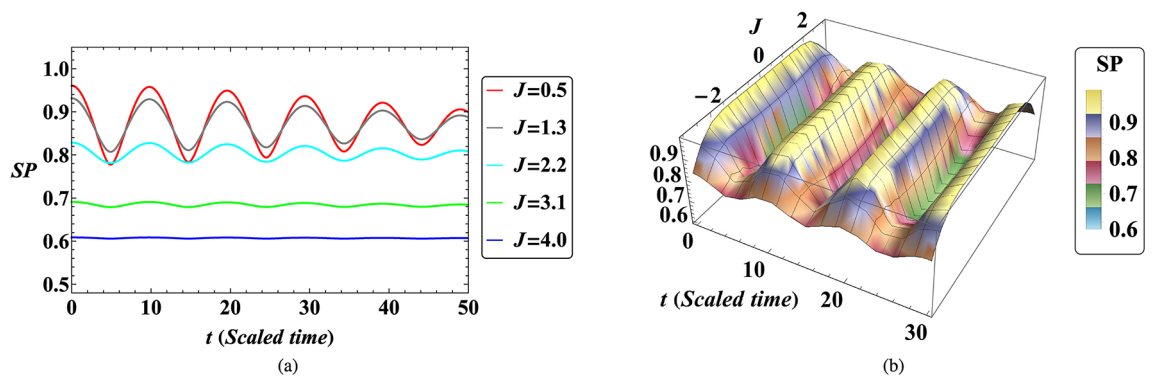
Figure 5. The time evolution of success probability SP of quantum two-qubit teleportation with increasing the homogeneous component of the magnetic field B when (**a**) $J = 1.2, K_z = 4.8, D_z = 2,$ $\Delta_z = 1, \Delta_Q = 0.3, \lambda = 0.1, \delta_0 = 1, \theta = \pi/2, \varphi = \pi, T = 0.8$ and (**b**) the contour plot B vs t when $J = 1.1, K_z = 3.8, D_z = 2, \Delta_z = 1, \Delta_Q = 0.1, \lambda = 0.09, \delta_0 = 1, \theta = \pi/2, \phi = \pi, T = 0.4$.
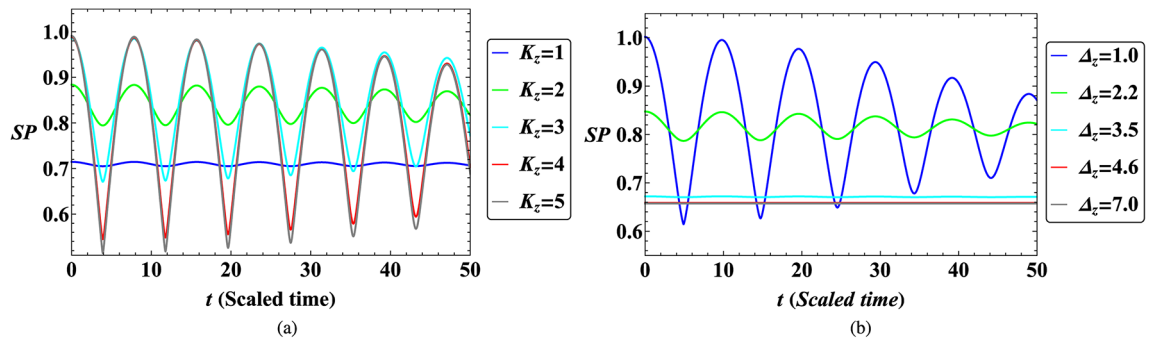
Figure 6. The qualitative behavior of success probability SP of quantum two-qubit teleportation with increasing (**a**) the KSEWA interaction strength K_z when $B = J = D_z = \Delta_z = T = \delta_0 = 1,$ $\Delta_Q = \lambda = 0.1, \theta = \pi/2, \phi = \pi$ and (**b**) the anisotropy coupling constant Δ_z when $B = 0.4, J = 1.15, K_z = 3.7, D_z = 1.5\Delta_Q = 0.2, \lambda = 0.08, \delta_0 = 1, \theta = \pi/2, \phi = \pi, T = 0.85$.

Figure 7. The time evolution of success probability SP of quantum two-qubit teleportation with increasing the strength of the Heisenberg exchange interaction J when (**a**) $B = 0.6, K_z = 4.2, D_z = 3,$ $\Delta_z = 1, \Delta_Q = 0.2, \lambda = 0.08, \delta_0 = 1, \theta = \pi/2, \phi = \pi, T = 0.9$ and (**b**) $B = 1.05, K_z = 4.7, D_z = 3,$ $\Delta_z = 0.9, \Delta_Q = 0.0.063, \lambda = 0.08, \delta_0 = 1, \theta = \pi/2, \phi = \pi, T = 0.7$.

the value of the SP decreases. Hence, in contrast to Fig. 6b, quantum teleportation based on the current hybrid channel is negatively affected by the anisotropy coupling.

Moreover, the temporal variations of the SP with amplifying the spin-spin exchange interaction J are depicted in Fig. 7. We can derive the result that for the $J > 0$ which represents the interaction of the antiferromagnetic

between the spin sites, with rising the J the qualitative behavior of the SP decreases. But, for $J < 0$ which represents the interaction of the ferromagnetic between the spin sites, the contrary result is obtained.

At last, the temporal variations of the *SP* for various values of the strength of the DM interaction D_z is plotted in Fig. 8a. The findings from this figure indicate that with the increase in the strength of the interaction D_z, the value of *SP* decreases. In addition, it can be seen that when the values of D_z and K_z become the same, the oscillations of *SP* behavior are suppressed, and the value of *SP* decreases. Besides, the qualitative behavior of the *SP* versus D_z and K_z at the initial time $t = 1$ for two-qubit quantum teleportation is illustrated in Fig. 8b. Here, we see that the same values of the D_z and K_z lead to the suppression of the *SP* in the two-qubit quantum teleportation based on the current model.

Conclusion

Investigating the performance of different channels and examining the success of quantum teleportation is an essential task in quantum communication. In this paper, we theoretically investigate the feasibility of quantum two-qubit teleportation based on a hybrid channel including two-spin of XXZ Heisenberg chain influenced by an external homogeneous magnetic field characterized by Dzyaloshinskii-Moriya (DM) interaction, Kaplan-Shekhtman-Entin-Wohlman-Aharony (KSEWA) interaction, and anisotropy interaction. In detail, the hybrid channel proposed here refers to the two-spin system simultaneously influenced by a thermal, magnetic, and classical channel that contains classical static noise. This hybrid channel allowed us to investigate various possibilities, including the simultaneous investigation of several interactions, thermal and magnetic effects, and the effects of classical static noise at the same time corresponding to the evolution of the system in quantum teleportation that it is very valuable in the practical implementation of quantum teleportation.

To study the quality of quantum two-qubit teleportation based on a current hybrid channel, we used the criteria of success probability (SP), fidelity (f), and average fidelity (f_{av}). The main focus of this work was on the qualitative behavior of the SP for the quantum two-qubit teleportation. Furthermore, we considered that the important information has been encoded in the phase of the initial qubit state and Alice transferred the quantum state to Bob. We report on the quantum phase estimation using Hilbert-Schmidt speed (HSS) in quantum teleportation based on the presented model. We illustrate how adjusting system parameters can achieve improved quantum teleportation performance within this framework.

In particular, by decreasing the static noise control parameter we achieved a stable SP, fidelity, average fidelity, and quantum phase estimation according to this hybrid channel over a long time for the faithful quantum two-qubit teleportation. Furthermore, the quantum teleportation based on a hybrid channel under the effect of the KSEWA interaction is improved. On the contrary, the quantum teleportation under the effect of the anisotropy coupling is disturbed. Moreover, we derived the result that for the $J > 0$ which represents the interaction of the antiferromagnetic between the spin sites, with rising the J the quantum teleportation can be disturbed. But, for $J < 0$ which represents the interaction of the ferromagnetic between the spin sites, the contrary result is obtained. One outcome is that when the strength of DM and KSEWA interactions are equal, the success probability of two-qubit teleportation in the current model reaches its minimum. This finding could inspire additional exploration of the hybrid channel in quantum communication. Finally, corresponding to system parameters, we illustrated that this hybrid channel based on the current model has a good potential to be successful in quantum teleportation.

Another significant finding was our introduction of a robust witness for identifying non-Markovian behavior in system dynamics and quantum memory effects, utilizing success probability, which can rival the effectiveness of trace distance. Based on this witness, we assessed the non-Markovian effects in the quantum teleportation process. We demonstrated that during certain time intervals, the suggested hybrid channel distinctly exhibited the non-Markovian effects.

This article can be motivation for the implementation of different hybrid channels in quantum communication to improve the quantum state transformation. Our findings could potentially address persistent challenges in
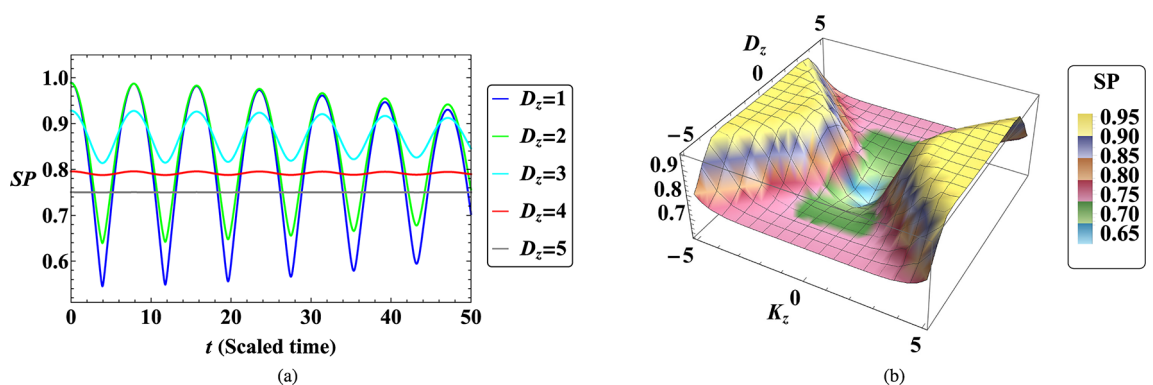
Figure 8. (**a**) The temporal evolution of success probability *SP* of two-qubit quantum teleportation with increasing the strength of theDM interaction D_z when $B = 1, J = 1, K_z = 4, \Delta_z = 1, \Delta_Q = 0.1, \lambda = 0.1, \delta_0 = 1, \theta = \pi/2, \phi = \pi, T = 1$, and (**b**) the qualitative behavior of the *SP* versus D_z and K_z when $B = 1, J = 1, \Delta_z = 1, \Delta_Q = 0.1, \lambda = 0.1, \delta_0 = 1, \theta = \pi/2, \phi = \pi, T = 1, t = 1$.

achieving reliable quantum teleportation over extended distances, thereby enhancing various applications such as information security[105], quantum remote sensing[106], quantum network[7], radar[107], lidar[108], imaging[109], antenna design[110], navigation[111], and quantum computing system[83].

Data availibility statement

All data generated or analyzed during this study are included in this paper.

References

1. Bennett, C. H. et al. Teleporting an unknown quantum state via dual classical and Einstein–Podolsky–Rosen channels. *Phys. Rev. Lett.* **70**, 1895 (1993).
2. Boschi, D., Branca, S., De Martini, F., Hardy, L. & Popescu, S. Experimental realization of teleporting an unknown pure quantum state via dual classical and Einstein–Podolsky–Rosen channels. *Phys. Rev. Lett.* **80**, 1121 (1998).
3. Bouwmeester, D. et al. Experimental quantum teleportation. *Nature* **390**, 575 (1997).
4. Gisin, N. & Thew, R. Quantum communication. *Nat. Photon.* **1**, 165 (2007).
5. Gruska, J., et al. Quantum computing, Vol. 2005 (McGraw-Hill London, 1999).
6. Yonezawa, H., Aoki, T. & Furusawa, A. Demonstration of a quantum teleportation network for continuous variables. *Nature* **431**, 430 (2004).
7. Hermans, S. et al. Qubit teleportation between non-neighbouring nodes in a quantum network. *Nature* **605**, 663 (2022).
8. Pirandola, S., Eisert, J., Weedbrook, C., Furusawa, A. & Braunstein, S. L. Advances in quantum teleportation. *Nat. Photon.* **9**, 641 (2015).
9. Ali, L., Ikram, M., Abbas, T. & Ahmad, I. Teleportation of atomic external states on the internal degrees of freedom. *Quant. Inf. Process.* **21**, 55 (2022).
10. Zidan, N., Ur Rahman, A. & Haddadi, S. Quantum teleportation in a two-superconducting qubit system under dephasing noisy channel: role of Josephson and mutual coupling energies. *Laser Phys. Lett.* **20**(2), 025204 (2023).
11. Hosseiny, S. M. Quantum dense coding and teleportation based on two coupled quantum dot molecules influenced by intrinsic decoherence, tunneling rates, and Coulomb coupling interaction. *Appl. Phys. B* **130**, 8 (2024).
12. Hosseiny, S. M. Quantum teleportation and phase quantum estimation in a two-qubit state influenced by dipole and symmetric cross interactions. *Phys. Scr.* **98**, 115101 (2023).
13. Raussendorf, R. & Briegel, H. J. A one-way quantum computer. *Phys. Rev. Lett.* **86**, 5188 (2001).
14. Sangouard, N., Simon, C., De Riedmatten, H. & Gisin, N. Quantum repeaters based on atomic ensembles and linear optics. *Rev. Modern Phys.* **83**, 33 (2011).
15. Gottesman, D. & Chuang, I. L. Demonstrating the viability of universal quantum computation using teleportation and single-qubit operations. *Nature* **402**, 390 (1999).
16. Ursin, R. et al. Quantum teleportation across the Danube. *Nature* **430**, 849 (2004).
17. Jin, X.-M. et al. Experimental free-space quantum teleportation. *Nat. Photon.* **4**, 376 (2010).
18. Kim, Y.-H., Kulik, S. P. & Shih, Y. Quantum teleportation of a polarization state with a complete Bell state measurement. *Phys. Rev. Lett.* **86**, 1370 (2001).
19. Yin, J. et al. Quantum teleportation and entanglement distribution over 100-kilometre free-space channels. *Nature* **488**, 185 (2012).
20. Ma, X.-S. et al. Quantum teleportation over 143 kilometres using active feed-forward. *Nature* **489**, 269 (2012).
21. Marcikic, I., De Riedmatten, H., Tittel, W., Zbinden, H. & Gisin, N. Long-distance teleportation of qubits at telecommunication wavelengths. *Nature* **421**, 509 (2003).
22. De Riedmatten, H. et al. Long distance quantum teleportation in a quantum relay configuration. *Phys. Rev. Lett.* **92**, 047904 (2004).
23. Landry, O., van Houwelingen, J. A. W., Beveratos, A., Zbinden, H. & Gisin, N. Quantum teleportation over the Swisscom telecommunication network. *JOSA B* **24**, 398 (2007).
24. Metcalf, B. J. et al. Quantum teleportation on a photonic chip. *Nat. Photon.* **8**, 770 (2014).
25. Wang, X.-L. et al. Quantum teleportation of multiple degrees of freedom of a single photon. *Nature* **518**, 516 (2015).
26. Nielsen, M. A., Knill, E. & Laflamme, R. Complete quantum teleportation using nuclear magnetic resonance. *Nature* **396**, 52 (1998).
27. Furusawa, A. et al. Unconditional quantum teleportation. *Science* **282**, 706 (1998).
28. Bowen, W. P. et al. Experimental investigation of continuous-variable quantum teleportation. *Phys. Rev. A* **67**, 032302 (2003).
29. Zhang, T. C., Goh, K., Chou, C., Lodahl, P. & Kimble, H. J. Quantum teleportation of light beams. *Phys. Rev. A* **67**, 033802 (2003).
30. Takei, N., Yonezawa, H., Aoki, T. & Furusawa, A. High-fidelity teleportation beyond the no-cloning limit and entanglement swapping for continuous variables. *Phys. Rev. Lett.* **94**, 220502 (2005).
31. Yonezawa, H., Braunstein, S. L. & Furusawa, A. Experimental demonstration of quantum teleportation of broadband squeezing. *Phys. Rev. Lett.* **99**, 110503 (2007).
32. Takei, N. et al. Experimental demonstration of quantum teleportation of a squeezed state. *Phys. Rev. A* **72**, 042304 (2005).
33. Lee, N. et al. Teleportation of nonclassical wave packets of light. *Science* **332**, 330 (2011).
34. Yukawa, M., Benichi, H. & Furusawa, A. High-fidelity continuous-variable quantum teleportation toward multistep quantum operations. *Phys. Rev. A* **77**, 022314 (2008).
35. Takeda, S., Mizuta, T., Fuwa, M., Van Loock, P. & Furusawa, A. Deterministic quantum teleportation of photonic quantum bits by a hybrid technique. *Nature* **500**, 315 (2013).
36. Sherson, J. F. et al. Quantum teleportation between light and matter. *Nature* **443**, 557 (2006).
37. Krauter, H. et al. Deterministic quantum teleportation between distant atomic objects. *Nat. Phys.* **9**, 400 (2013).
38. Chen, Y.-A. et al. Memory-built-in quantum teleportation with photonic and atomic qubits. *Nat. Phys.* **4**, 103 (2008).
39. Bao, X.-H. et al. Quantum teleportation between remote atomic-ensemble quantum memories. *Proc. Natl. Acad. Sci.* **109**, 20347 (2012).
40. Barrett, M. et al. Deterministic quantum teleportation of atomic qubits. *Nature* **429**, 737 (2004).
41. Riebe, M. et al. Deterministic quantum teleportation with atoms. *Nature* **429**, 734 (2004).
42. Riebe, M. et al. Quantum teleportation with atoms: quantum process tomography. *New J. Phys.* **9**, 211 (2007).
43. Olmschenk, S. et al. Quantum teleportation between distant matter qubits. *Science* **323**, 486 (2009).
44. Nölleke, C. et al. Quantum teleportation between distant matter qubits. *Phys. Rev. Lett.* **110**, 140403 (2013).
45. Gao, W. et al. Quantum teleportation from a propagating photon to a solid-state spin qubit. *Nat. Commun.* **4**, 2744 (2013).
46. Bussières, F. et al. Quantum teleportation from a telecom-wavelength photon to a solid-state quantum memory. *Nat. Photon.* **8**, 775 (2014).

47. Steffen, L. et al. Deterministic quantum teleportation with feed-forward in a solid state system. *Nature* **500**, 319 (2013).
48. Pfaff, W. et al. Unconditional quantum teleportation between distant solid-state quantum bits. *Science* **345**, 532 (2014).
49. He, C. et al. Core-shell nanoscale coordination polymers combine chemotherapy and photodynamic therapy to potentiate checkpoint blockade cancer immunotherapy. *Nat. Commun.* **7**, 12499 (2016).
50. Kumar, A., Haddadi, S., Pourkarimi, M. R., Behera, B. K. & Panigrahi, P. K. Experimental realization of controlled quantum teleportation of arbitrary qubit states via cluster states. *Sci. Rep.* **10**, 13608 (2020).
51. Liu, Z.-D. et al. Experimental realization of high-fidelity teleportation via a non-Markovian open quantum system. *Phys. Rev. A* **102**, 062208 (2020).
52. Langenfeld, S. et al. Quantum teleportation between remote qubit memories with only a single photon as a resource. *Phys. Rev. Lett.* **126**, 130502 (2021).
53. Lago-Rivera, D., Rakonjac, J. V., Grandi, S. & Riedmatten, H. . D. . Long distance multiplexed quantum teleportation from a telecom photon to a solid-state qubit. *Nat. Commun.* **14**, 1889 (2023).
54. Hu, X. M., Guo, Y., Liu, B. H., Li, C. F. & Guo, G. C. Progress in quantum teleportation. *Nat. Rev. Phys.* **5**(6), 339–353 (2023).
55. Hu, M.-L. Teleportation of the one-qubit state in decoherence environments. *J. Phys. B: Atom. Mol. Opt. Phys.* **44**, 025502 (2011).
56. Hu, M.-L. Teleportation of the one-qubit state in decoherence environments. *Quant. Inf. Process.* **12**, 229 (2013).
57. Lee, J. & Kim, M. Entanglement teleportation via Werner states. *Phys. Rev. Lett.* **84**, 4236 (2000).
58. Oh, S., Lee, S. & Lee, H.-W. Fidelity of quantum teleportation through noisy channels. *Phys. Rev. A* **66**, 022316 (2002).
59. Jung, E. et al. Greenberger–Horne–Zeilinger versus W states: Quantum teleportation through noisy channels. *Phys. Rev. A* **78**, 012312 (2008).
60. Rao, D. B., Panigrahi, P. & Mitra, C. Teleportation in the presence of common bath decoherence at the transmitting station. *Phys. Rev. A* **78**, 022336 (2008).
61. Yeo, Y., Kho, Z.-W. & Wang, L. Effects of Pauli channels and noisy quantum operations on standard teleportation. *Europhys. Lett.* **86**, 40009 (2009).
62. Breuer, H.-P. & Petruccione, F. *The Theory of Open Quantum Systems* (Oxford University Press, USA, 2002).
63. Rivas, A., Huelga, S. F. Open quantum systems, Vol. 10 (Springer, 2012)
64. Cai, X. et al. Quantum dynamical speedup in a nonequilibrium environment. *Phys. Rev. A* **95**, 052104 (2017).
65. Cai, X. & Zheng, Y. Non-Markovian decoherence dynamics in nonequilibrium environments. *J. Chem. Phys.* **149**, 094107 (2018).
66. Cai, X. Quantum dephasing induced by non-Markovian random telegraph noise. *Sci. Rep.* **10**, 88 (2020).
67. Czerwinski, A. Quantum communication with polarization-encoded qubits under majorization monotone dynamics. *Mathematics* **10**, 3932 (2022).
68. Breuer, H.-P., Laine, E.-M. & Piilo, J. Measure for the degree of non-Markovian behavior of quantum processes in open systems. *Phys. Rev. Lett.* **103**, 210401 (2009).
69. Breuer, H.-P., Laine, E.-M., Piilo, J. & Vacchini, B. Colloquium: Non-Markovian dynamics in open quantum systems. *Rev. Modern Phys.* **88**, 021002 (2016).
70. Chen, H., Han, T., Chen, M., Ren, J., Cai, X., Meng, X., Peng, Y. Quantum state tomography in nonequilibrium environments. in Photonics, Vol. 10 (MDPI, 2023) p. 134
71. Rahman, A. U., Yang, M., Zangi, S. M. & Qiao, C. Probing a hybrid channel for the dynamics of non-local features. *Symmetry* **15**, 2189 (2023).
72. Omri, M., Abd-Rabbou, M., Khalil, E. & Abdel-Khalek, S. Thermal information and teleportation in two-qutrit Heisenberg XX chain model. *Alex. Eng. J.* **61**, 8335 (2022).
73. Koretsune, T., Kikuchi, T. & Arita, R. First-principles evaluation of the Dzyaloshinskii–Moriya interaction. *J. Phys. Soc. Japan* **87**, 041011 (2018).
74. Zheludev, A. et al. Experimental Evidence for Kaplan-Shekhtman–Entin–Wohlman–Aharony Interactions in $Ba_2CuGe_2O_7$. *Phys. Rev. Lett.* **81**, 5410 (1998).
75. Dahbi, Z., Rahman, A. U. & Mansour, M. Skew information correlations and local quantum Fisher information in two gravitational cat states. *Phys. A Stat. Mech. Appl.* **609**, 128333 (2023).
76. Dahbi, Z., Oumennana, M., Anouz, K. E., Mansour, M. & Allati, A. E. Quantum Fisher information versus quantum skew information in double quantum dots with Rashba interaction. *Appl. Phys. B* **129**, 27 (2023).
77. Nweke, N. et al. Experimental characterization of the separation between wavelength-multiplexed quantum and classical communication channels. *Appl. Phys. Lett.* **87**, 174103 (2005).
78. Hosur, P., Qi, X.-L., Roberts, D. A. & Yoshida, B. Chaos in quantum channels. *J. High Energy Phys.* **2016**, 1 (2016).
79. Khanna, V. K, Khanna, V. K. Short-channel effects in MOSFETs. in Integrated Nanoelectronics: Nanoscale CMOS, Post-CMOS and Allied Nanotechnologies , p. 73 (2016)
80. Neuber, A., Butcher, M., Hatfield, L. & Krompholz, H. Electric current in DC surface flashover in vacuum. *J. Appl. Phys.* **85**, 3084 (1999).
81. De Vega, I. & Alonso, D. Dynamics of non-Markovian open quantum systems. *Rev. Modern Phys.* **89**, 015001 (2017).
82. Hesabi, S. & Afshar, D. Non-Markovianity measure of Gaussian channels based on fidelity of teleportation. *Phys. Lett. A* **410**, 127482 (2021).
83. Liu, T. The applications and challenges of quantum teleportation. in Journal of Physics: Conference Series, Vol. 1634 (IOP Publishing, 2020) p. 012089
84. Nakahara, M., Ohmi, T. Quantum computing: from linear algebra to physical realizations (CRC press, 2008)
85. Bowen, G. & Bose, S. Teleportation as a depolarizing quantum channel, relative entropy, and classical capacity. *Phys. Rev. Lett.* **87**, 267901 (2001).
86. Jahromi, H. R. Remote sensing and faithful quantum teleportation through non-localized qubits. *Phys. Lett. A* **424**, 127850 (2022).
87. Nielsen, M. A., Chuang, I. L. Quantum computation and quantum information. Quantum computation and quantum information (Cambridge university press, 2010)
88. Laine, E.-M., Piilo, J. & Breuer, H.-P. Measure for the non-Markovianity of quantum processes. *Phys. Rev. A* **81**, 062115 (2010).
89. Gessner, M. & Smerzi, A. Statistical speed of quantum states: Generalized quantum Fisher information and Schatten speed. *Phys. Rev. A* **97**, 022109 (2018).
90. Rangani Jahromi, H. & Lo Franco, R. Hilbert-Schmidt speed as an efficient figure of merit for quantum estimation of phase encoded into the initial state of open n-qubit systems. *Sci. Rep.* **11**(1), 7128 (2021).
91. Jahromi, H. R., Mahdavipour, K., Shadfar, M. K. & Franco, R. L. Witnessing non-Markovian effects of quantum processes through Hilbert-Schmidt speed. *Phys. Rev. A* **102**, 022221 (2020).
92. Deffner, S. & Lutz, E. Quantum speed limit for non-Markovian dynamics. *Phys. Rev. Lett.* **111**, 010402 (2013).
93. Mirkin, N., Toscano, F. & Wisniacki, D. A. Quantum-speed-limit bounds in an open quantum evolution. *Phys. Rev. A* **94**, 052125 (2016).
94. Liu, H.-B., Yang, W., An, J.-H. & Xu, Z.-Y. Mechanism for quantum speedup in open quantum systems. *Phys. Rev. A* **93**, 020105 (2016).
95. Ahansaz, B. & Ektesabi, A. Quantum speedup, non-Markovianity and formation of bound state. *Sci. Rep.* **9**, 14946 (2019).
96. Wu, S.-X. & Yu, C.-S. Quantum speed limit for a mixed initial state. *Phys. Rev. A* **98**, 042132 (2018).

97. Zou, H.-M., Liu, R., Long, D., Yang, J. & Lin, D. Ohmic reservoir-based non-Markovianity and quantum speed limit time. *Phys. Scr.* **95**, 085105 (2020).
98. Haseli, S., Salimi, S. & Khorashad, A. A measure of non-Markovianity for unital quantum dynamical maps. *Quant. Inf. Process.* **14**, 3581 (2015).
99. Oumennana, M., Rahman, A. U. & Mansour, M. Quantum coherence versus non-classical correlations in XXZ spin-chain under Dzyaloshinsky-Moriya (DM) and KSEA interactions. *Appl. Phys. B* **128**, 162 (2022).
100. Rahman, A. U., Khedif, Y., Javed, M., Ali, H. & Daoud, M. Characterizing two-qubit non-classical correlations and non-locality in mixed local dephasing noisy channels. *Annalen der Physik* **534**, 2200197 (2022).
101. Sakurai, J. J., Commins, E. D. Modern quantum mechanics, revised edition, Modern quantum mechanics, revised edition (1995)
102. Tchoffo, M., Kenfack, L. T., Fouokeng, G. C. & Fai, L. C. Quantum correlations dynamics and decoherence of a three-qubit system subject to classical environmental noise. *Eur. Phys. J. Plus* **131**, 1 (2016).
103. Rahman, A. U., Noman, M., Javed, M., Ullah, A. & Luo, M.-X. Effects of classical fluctuating environments on decoherence and bipartite quantum correlation dynamics. *Laser Phys.* **31**, 115202 (2021).
104. Mohr, P. J. & Phillips, W. D. Dimensionless units in the SI. *Metrologia* **52**, 40 (2014).
105. Okane, H., Hakoshima, H., Takeuchi, Y., Seki, Y. & Matsuzaki, Y. Quantum remote sensing under the effect of dephasing. *Phys. Rev. A* **104**, 062610 (2021).
106. Yin, P. et al. Experimental demonstration of secure quantum remote sensing. *Phys. Rev. Appl.* **14**, 014065 (2020).
107. Bowell, R. A., Brandsema, M. J., Ahmed, B. M., Narayanan, R. M., Howell, S. W., Dilger, J. M. Electric field correlations in quantum radar and the quantum advantage .in Radar Sensor Technology XXIV, Vol. 11408 (SPIE, 2020) pp. 137–150
108. M. J. Brandsema, R. M. Narayanan, & M. Lanzagorta, Correlation properties of single photon binary waveforms used in quantum radar/lidar. in Radar sensor technology XXIV, Vol.11408 (SPIE, 2020) pp. 113–126
109. Sebastianelli, A., Zaidenberg, D. A., Spiller, D., Le Saux, B. & Ullo, S. L. On circuit-based hybrid quantum neural networks for remote sensing imagery classification. *IEEE J. Sel. Top. Appl. Earth Observ. Remote Sens.* **15**, 565–580 (2021).
110. Slepyan, G. Y., Vlasenko, S. & Mogilevtsev, D. Quantum antennas. *Adv. Quant. Technol.* **3**, 1900120 (2020).
111. Fancher, C. T., Scherer, D. R., John, M. C. S. & Marlow, B. L. S. Rydberg atom electric field sensors for communications and sensing. *IEEE Trans. Quant. Eng.* **2**, 1 (2021).

Author contributions

Practical research was conducted by S.M.H. and M.N. Interpretations and comparison of results and writing of the article were done by S.M.H. and M.N. with the help of J.S.Y. The article was reviewed and edited by J.S.Y.

Declarations

Competing interests

The authors declare no competing interests.

Additional information

Correspondence and requests for materials should be addressed to S.M.H. or J.S.-Y.

Reprints and permissions information is available at www.nature.com/reprints.

Publisher's note Springer Nature remains neutral with regard to jurisdictional claims in published maps and institutional affiliations.